Electrostatic Effect on the Flow Behavior of a Dilute Gas/Cohesive Particle Flow System

Yu-Feng Zhang, Yi Yang, and Hamid Arastoopour
Dept. of Chemical and Environmental Engineering, Illinois Institute of Technology, Chicago, IL 60616

Cohesive (Group C) particles have been widely used in various industries. To handle and process such fine particles, a clear understanding of the flow behavior and interparticle force, is needed. To achieve that objective, a Laser Doppler Anemometer system was used to measure particle velocity, fluctuating velocity, and size and extent of agglomeration or cluster formation of particles in a dilute gas/fine oil shale particle flow system with particle density of 2,082 kg/m^3, average particle volumetric concentration of 1.5%, and average particle mass flux of about 100 kg/m^2·s in a controlled-moisture environment. The flow behavior of the particles was also studied for a mixture of 99% shale particles and 1% antistatic agent (Larostat powder, a quaternary ammonium compound) to examine the role of electrostatic force in gas/cohesive particle flow behavior. The addition of Larostat powder significantly reduced the electrostatic force and, in turn, made Group C particles behave similar to Group A or in some cases to Group B particles. In addition, our experimental data showed that the Maxwellian distribution function is a reasonable assumption to describe the velocity probability density function of the shale particles with or without antistatic agents.

Introduction

Gas/cohesive particle flow systems have been widely used in the energy, chemical, pharmaceutical, and material processing industries. Interest in using advanced experimental techniques to understand flow behavior is increasing. Optical instruments are among the most promising measurement techniques for dilute gas-solid flow systems. Soo et al. (1964) was the first to use optical fiber to measure particle concentration. Reddy (1967) used the sterophotogrammetry method to obtain information about particle motion in a vertical pipe. Lesinski et al. (1981) and Tsuji et al. (1981, 1984) simultaneously measured air and particle velocities by setting threshold values against the pedestal and Doppler components of the photomultiplier signal. Farmer (1978) attempted to obtain information regarding particle size and velocity. Arastoopour and Yang (1991) conducted preliminary measurements of cohesive particle flow behavior in dilute gas/particle flow systems using laser doppler anemometry.

Cohesive particles (Group C) (Geldart, 1973) form rather large clusters or agglomerates in gas/particle flow systems or reactors due to relatively high interparticle forces. As a result of this, solid-phase flow characteristics such as mixing, residence time, residence time distribution, or conversion may be changed significantly. The formation of agglomerates and clusters is influenced by many factors such as gas velocity, moisture content of the particle, and electrostatic force.

In spite of the important role that electrostatic force plays in the flow of particles, particularly for Groups A and C particles, there are only a few quantitative studies available in the literature. This could be mainly due to the complexity of the problem and the difficulty of particle flow measurement in such systems. The objective of this study, which is an extension of the work of Arastoopour and Yang (1991), was to obtain a comprehensive and complete study of the effect of electrostatic force on cohesive particles. To achieve our goal, a laser doppler anemometry system was used to measure flow behavior and the extent of agglomeration or cluster formation in a dilute gas/fine oil shale particle flow system in a controlled-moisture environment. The flow behavior of the particles was also studied for a mixture of 99% shale particles and 1% Larostat powder to obtain a better understanding of the role of electrostatic force in gas/fine particle flow behavior. The addition of Larostat powder significantly reduces the electrostatic force between the particles and between the particles and the wall.

Experimental setup

A dilute gas/particle circulating flow system and a laser doppler anemometry system have been developed with the capability of making detailed measurements of flow characteristics. This system developed by Yang (1991) was capable of measuring the radial profiles of the axial, mean and fluctuating velocities as well as the density and pressure drop distributions along the riser.

The circulating fluidized-bed system consists of six major parts: (1) a moisture controller with the capability to control the moisture content of the air under 5% relative humidity. The degree of humidity significantly influences the cohesiveness of the fine particles; (2) the main gas inlet which delivers dry air into the system; (3) a solid feeding section consisting of a screw feeder and a jet pump; (4) a 60-cm-long mixing chamber to obtain a more uniform particle/gas mixture; (5) a riser and test section which consist of a 2.75-m, clear, 5.08-cm-ID PVC pipe. The test section was located after the 1.07-cm acceleration or developing zone and was mounted with a pair of optical-glass windows to allow the laser beam to go through with minimum scattering; (6) the cyclones and recirculation and standpipe section which collect the particles and recirculate them back to the system through two standpipes (Figure 1).

Laser doppler anemometry (LDA) measurements

Velocity Measurement. Light scattered by a moving body is "doppler" shifted in frequency. By measuring this frequency shift, the velocity of the moving body may be determined. Based on this principle, we measured the velocity of particles passing through the focusing volume.

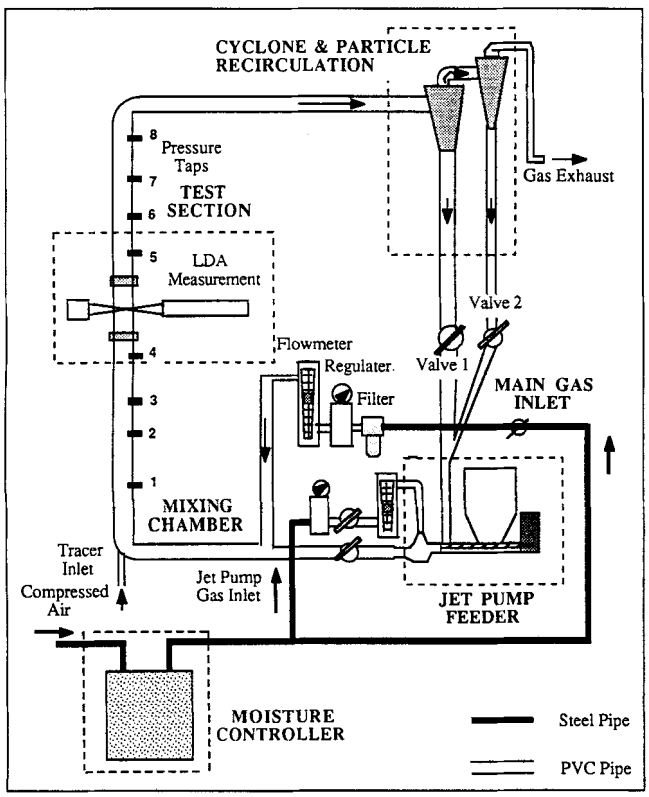

Figure 1. Experimental setup.

A laser beam from a Helium-Neon laser (15 mW at a wavelength of 6,328Å) is split by a beam splitter into two equal intensity beams (50 mm apart). After passing through a focusing lens of 250-mm focal length, these two beams intersect at the measuring point and generate the fringe pattern within the focusing volume. When a moving particle passes through this fringe area, the intensity of the scattered light from the particle surface varies with time to form the Doppler burst signal. This Doppler burst is received by the photodetector and its frequency is proportional to the velocity of the moving particle. Our computer program calculates the velocity and velocity fluctuation of each particle from the frequency measured by the LDA.

Particle-Size Distribution Measurement. It can be demonstrated theoretically that the shape of the Doppler burst signal is determined by the size, shape, and surface properties of the particle, as well as the optical system alignment and the actual path that the particle takes as it passes through the focusing volume.

In this study, we used the procedure developed by Arastoopour and Yang (1991) to estimate the particle size based on the amplitude of the Doppler signal.

The focusing volume of our LDA is an oval with two axes of 184 microns and 1,890 microns, respectively. The fringe space d_f is 3.2 μm. Light intensity is not uniformly distributed across the focusing volume. It is basically a Gaussian distribution which results in additional complexity of the Doppler signal. Arastoopour and Yang (1991) considered this effect in their procedure. Two criteria were used to discriminate the noise: (a) time criterion based on the reasonable Doppler signals duration time; (b) period criterion based on the appropriate level for relative standard deviation of the oscillating period in each Doppler burst.

To perform the particle-size information analysis, we used an HP5404 digitizing oscilloscope to record the Doppler signals which were then transferred to a PC for data processing. The signal amplitude received was translated to particle size using a calibration curve. The calibration curve was developed at the reference condition of 0.2 m/s superficial gas velocity for the case of 75 g of shale particles (0.15% particle volumetric concentration) with 1% Larostat powder and no agglomeration. At this condition, the amplitude vs. cumulative number percentage was compared with particle size vs. cumulative number percentage using the Coulter counter to obtain the signal amplitude vs. particle-size calibration curve (see Yang (1991) for more details). The volume average diameter of the particles was measured as 13.8 μm, and the number average diameter of the particles was measured as 1.5 μm using the Coulter counter.

Experimental procedures and measurements

First, all the filters were checked to ensure that the cores were clean and dry, and ice was fed into the moisture controller. Then the gas inlet valve was opened and the system was run for a short time without solid particles. The desired amount of solid particles was put into the hopper in the feeding system. After that, the solid feeder pump was turned on for a short time to inject the desired amount of solid particles into the system. The gas/particle mixture passed through the mixing and the acceleration zones; then the flow parameters

were measured using the laser doppler anemometer in the test section. The particles were separated from the gas and recirculated back to the feeding system via a two-stage cyclone located on the top of the experimental setup. Meanwhile, the gas was exhausted to the atmosphere. Several steady-state operating conditions at different solid loadings were obtained by adjusting the gas flow rates.

Two samples were prepared for the test. One was 750 g of shale particles and the other sample was 742.5 g of shale particles mixed with 1% Larostat powder (7.5 g). The addition of Larostat powder can eliminate or reduce the electrostatic force between particles and between the particles and the wall.

The 750 g of shale particles is equivalent to about 1.5% volumetric concentration and 100 kg/m^2·s solid mass flux. The outlet gas volumetric flow rate was set at different flow rates ranging from 1.9 to 8.5 L/s corresponding to 1.85 to 4.50 m/s superficial velocity. The gas flow rate was higher than the measured value of the outlet gas flow rate because the additional circulated gas accumulates in the vertical line. Yang (1991) measured the gas-phase axial velocity across the pipe and developed a relationship between outlet gas flow rate vs. superficial gas velocity. Yang's (1991) graph was used to obtain superficial gas velocity whenever it was necessary.

Electrostatic charge and antistatic agents

The generation of electrostatic charge in fine powder flow systems such as pneumatic conveying lines results from the separation of positive and negative charges due to frictional contact of individual particles with the wall (known as triboelectrification). During mechanical contact of the boundary between two dissimilar materials (such as particles and the wall of the pipe), some of the electrons in the material with the lower work function are pulled across the interface, thus creating a charge imbalance. When the particles are separated from the wall, this charge imbalance results in a net positive or negative particle charge. Triboelectrification is further complicated since magnitude and the sign of the net charge depend on the particle size (Jones and King, 1991).

The troublesome effects of static charging may become very serious and dangerous and, in some cases, can even result in an explosion. Since static electricity is a surface phenomenon, static charges may be best dissipated via decreasing the surface resistivity by adding antistatic agents.

In this study, we have used a cationic surfactant named Larostat 519 powder which is made of about 60% soyadimethylethyl-ammonium and 40% ethasulfate/amorphous Silica. Larostat is a nonflammable white powder with bulk density of 520 kg/m^3. This antistatic powder was added to oil shale particles to reduce the tendency for static buildup at the particle surface. In addition, Larostat particles act as slip agents, lowering the friction between particles and between the particles and the wall.

Results and Discussion

Particle velocity

The axial velocity at different radial locations for 750 g shale fines and shale fines with 1% Larostat powder circulating in the bed are shown in Figures 2 and 3, respectively.

For pure shale fines, it was found that there was an annular boundary region adjacent to the pipe wall. At low superficial gas velocities, the mean particle velocities approached zero between $r/R = 0.85$ and the wall. In addition, instantaneous reversal flow of particles was observed at the wall boundary with the average velocity of particles at approximately zero. The velocities of particles of different sizes first reached a maximum at about $r/R = 0.55$, then decreased to a minimum at $r/R = 0.25$, and then increased again around the center ($r/R = 0$). At high superficial gas velocities, the parti-

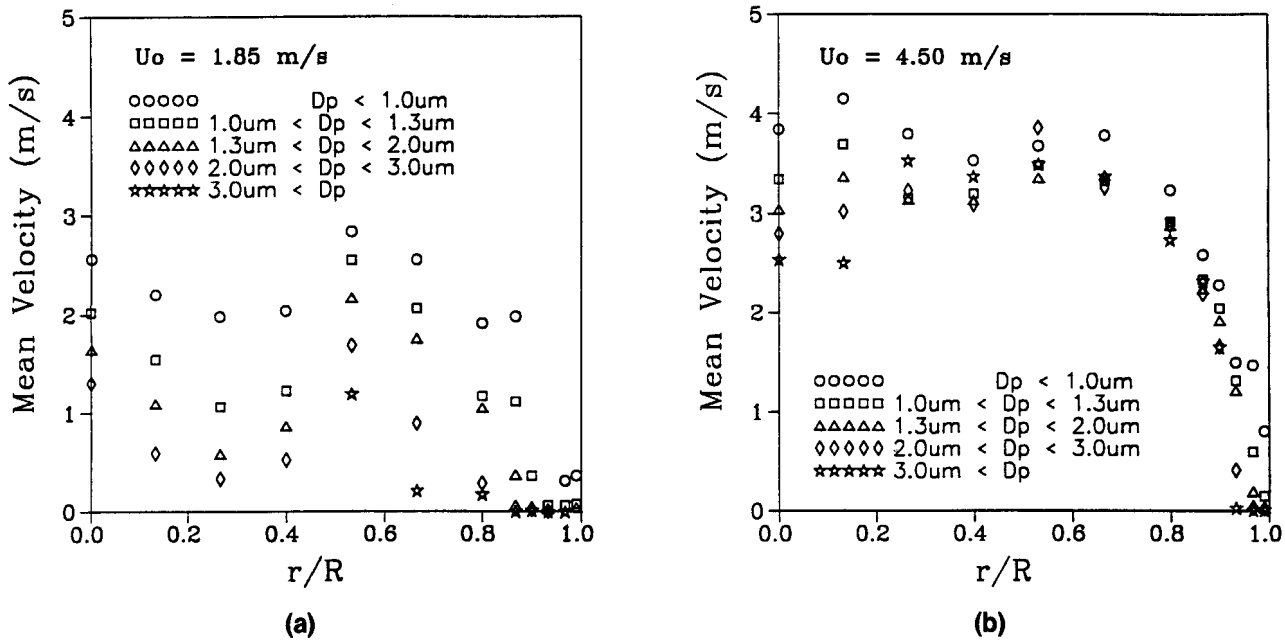

Figure 2. Mean radial distribution of axial velocity of 750 g of different sized shale particles at superficial gas velocity of: (a) 1.85 m/s; (b) 4.50 m/s.

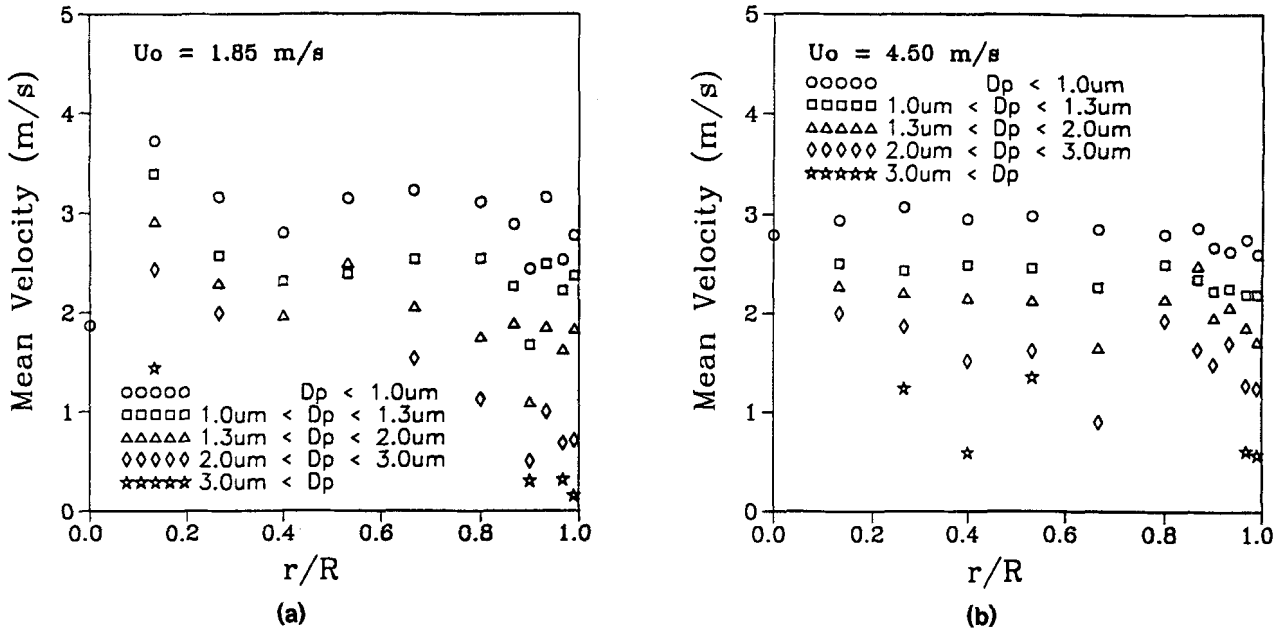

Figure 3. Mean radial distribution of axial velocity of 750 g mixture of 99% shale particles of different sizes and 1% Larostat particles at superficial gas velocity of: (a) 1.85 m/s; (b) 4.50 m/s.

cle velocities were parabolic in shape similar to the mean particle velocity measured by Yang et al. (1990). The particle velocities increased rapidly from very small values in the wall region to a maximum value at $r/R = 0.55$, then the velocities fluctuated slightly in the central region. The wall boundary region decreased with an increase in superficial gas velocity probably due to the increase in the number of collisions between the particles at the wall region and the particles in the core region.

For shale fines with 1% Larostat powder, at low superficial gas velocities, a minimum velocity was obtained at $r/R = 0.4$. In spite of the decrease in particle velocities near the wall, no stationary particles or instantaneous reversal flows were observed. At high superficial gas velocities, the mean velocity profiles of the small-size particles were almost flat. Only the large-size particle velocities decreased slightly near the wall due to collisions with the wall. This resulted in a plug-flow pattern with almost no specific wall regions. Adding Larostat powder significantly reduced interparticle force which resulted in the flatter profile for particle velocities. This information, which is actually important for large-scale reactor design and operation, showed how Group C particles may perform similar to Group B particles by eliminating interparticle force.

Tsuji et al. (1984) measured the air and particle velocities of Group B particles in a vertical 30-mm-ID pipe by using laser doppler velocimetry. Similar to our data, they found that the particle velocity distributions were flatter than the air velocity distributions and the point of maximum velocity deviated from the pipe axis. Zhang and Arastoopour (1995) measured the FCC (Group A) particle velocity distributions and observed similar trends in particle velocity distributions and the location of the maximum velocity. The maximum velocity deviation from the pipe axis could be mainly caused by ossilation due to electrostatic force. Overall, this effect for shale fines with 1% Larostat powder was not observed since the particle flow behavior became similar to Groups A and B particles.

Figures 4 and 5 show the radial profiles of the particle fluctuating velocities with 750 g shale fines and shale fines with 1% Larostat powder as circulating particles, respectively. The fluctuating velocity at each location is defined as

$$U_f(r) = \frac{1}{N_{\text{sample}}(r)} \sum_{k=1}^{N_{\text{sample}}(r)} \sqrt{[U_k(r) - U_m(r)]^2} \qquad (1)$$

where U_k, U_m and U_f are the instantaneous, average and fluctuating velocities of the particles, respectively, at a specific radial location.

For pure shale fines, the fluctuating velocities had similar profiles as the corresponding mean velocity profiles. The fluctuating velocities increased with superficial gas velocities, and dropped to a very small value at the wall region. The decrease in fluctuating velocities and, in some cases, reversal flow at the wall region could be due to significantly lower particle frequency of collisions and lower gas drag force on agglomerated particles. On the other hand, the fluctuating velocities for small particles did not change at the wall since the gas drag force exerted on the small particles was larger than the gravitational force and, in turn, no reversal flow of smaller particles was observed. Similar behavior was observed for FCC particles by Zhang and Arastoopour (1995). Furthermore, larger particles exhibited more chaotic behavior than the smaller particles in the core region especially for high superficial gas velocities.

For shale fines with 1% Larostat powder, the fluctuating velocities had similar flat profiles (plug flow) for all superficial gas velocities due to lower interparticle (electrostatic) force. The larger particles had smaller fluctuating velocities

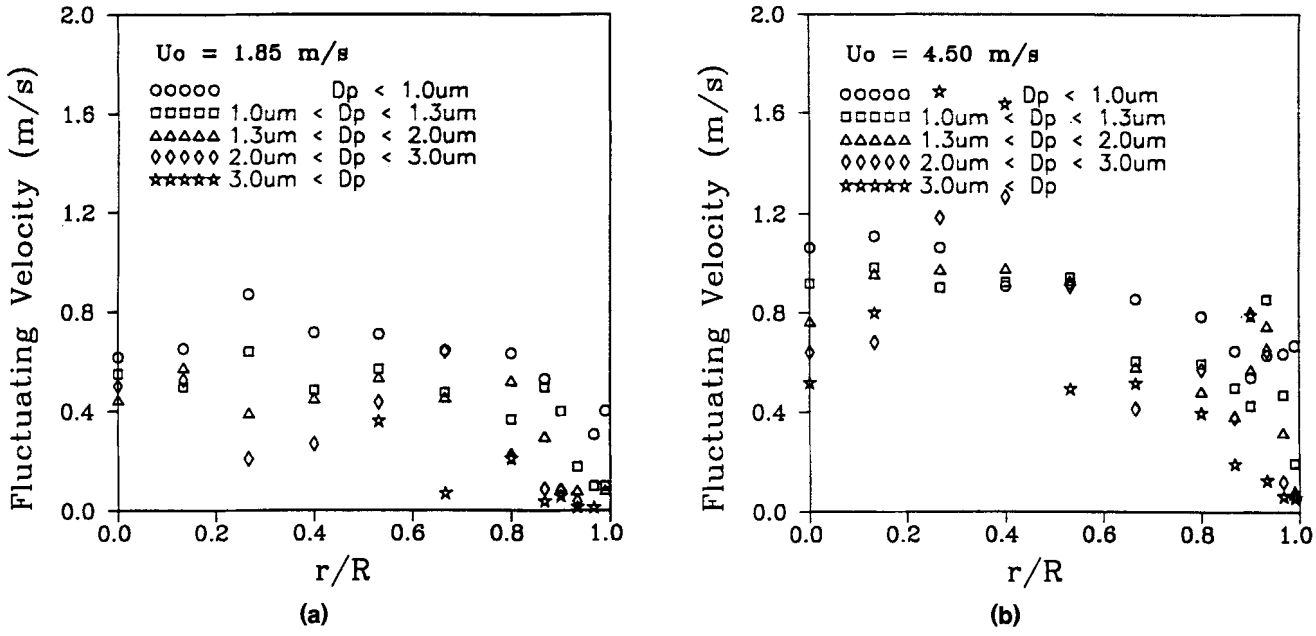

Figure 4. Radial profile of axial fluctuating velocity of 750 g of different sized shale particles at superficial gas velocity of: (a) 1.85 m/s; (b) 4.50 m/s.

near the wall, particularly at lower superficial gas velocities, probably due to less mixing and particle collision.

The turbulence intensity (U_f/U_m) at different radial locations for 750 g shale fines and shale fines with 1% Larostat powder circulating in the vertical line are shown in Figures 6 and 7, respectively.

For pure shale fines, the turbulence intensities of particles of different sizes were maximum at the wall and decreased to a minimum value at about $r/R = 0.6$, then increased and finally decreased slightly at the center. This behavior is similar to the mean velocities radial variation. Besides the wall region, turbulence intensity showed a maximum at about $r/R = 0.3$. This maximum was significantly smaller than the turbulence intensity value at the wall. The turbulence intensity in the wall region was much larger than in the central region, although the fluctuating velocity was smaller than in the core region. The fluctuating velocities in the wall region decreased and approached zero at the wall; however, the turbulence

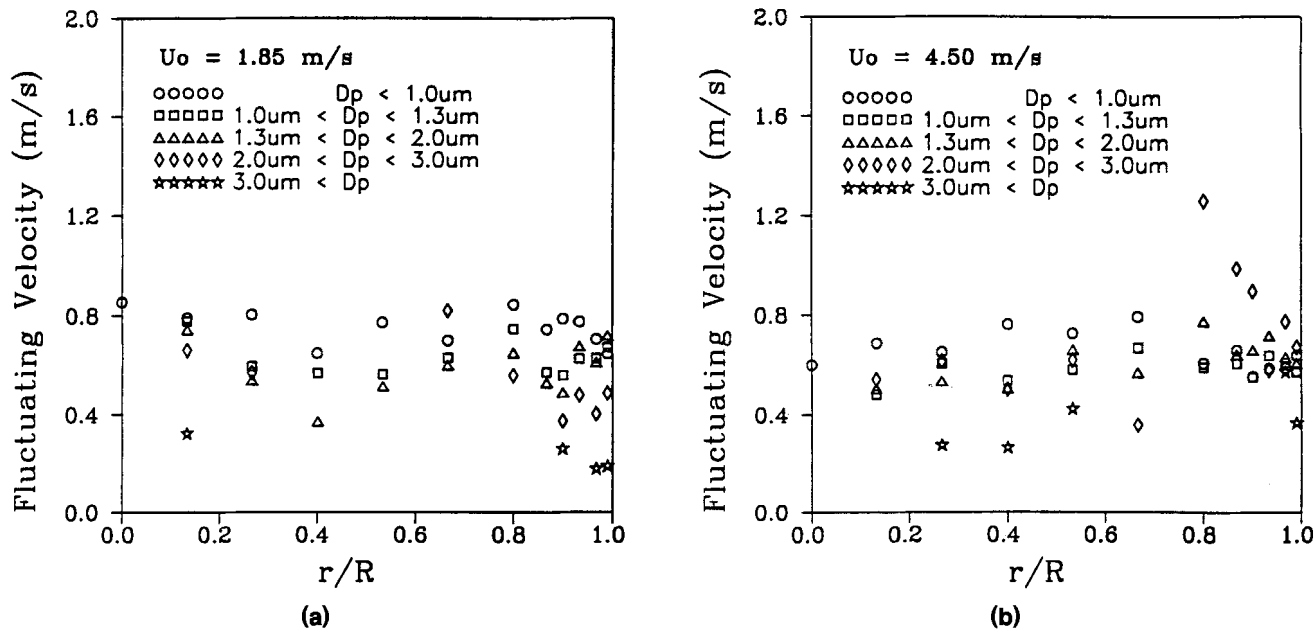

Figure 5. Radial profile of axial fluctuating velocity of 750 g mixture of 99% shale particles of different sizes and 1% Larostat particles at superficial gas velocity of: (a) 1.85 m/s; (b) 4.50 m/s.

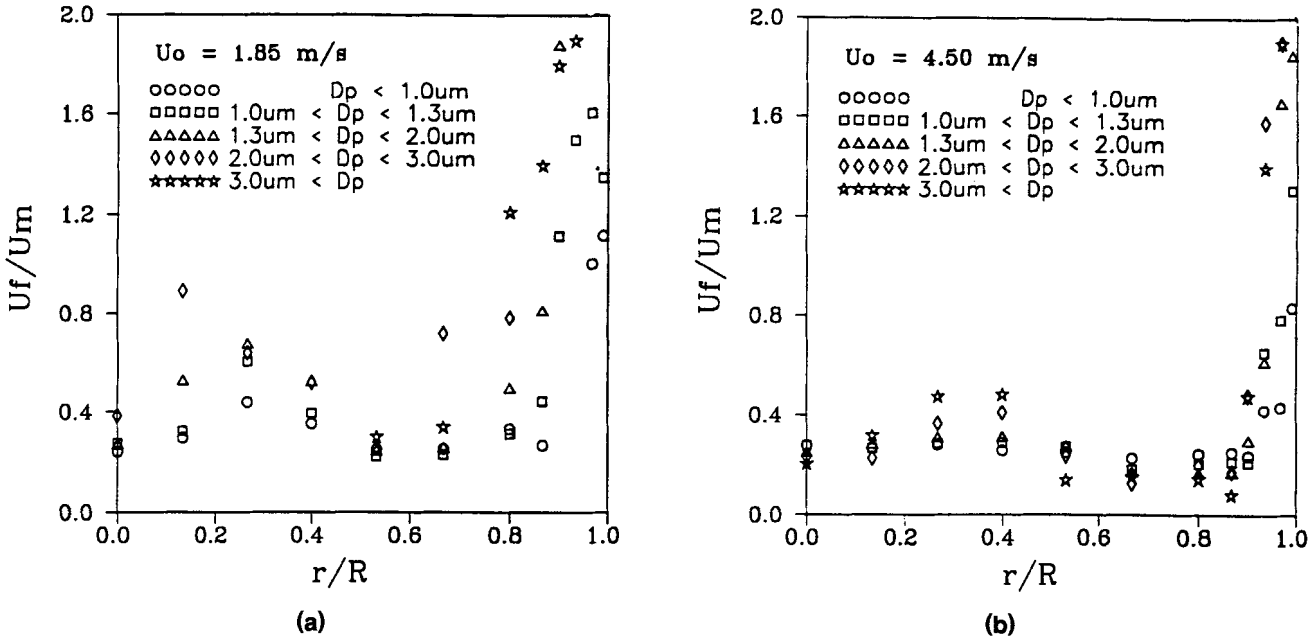

Figure 6. Radial profile of axial turbulent intensity of 750 g of different sized shale particles at superficial gas velocity of: (a) 1.85 m/s; (b) 4.50 m/s.

intensities increased significantly with maximum values very close to the wall because of the very small values of the particle velocities at this region.

For shale fines with 1% Larostat powder, the turbulence intensity profiles were flatter than for the pure shale particle flow cases. Only particles larger than 2 microns showed higher turbulence intensity near the wall. The Larostat powder reduced the electrostatic force effect especially near the wall such that particle collision became the dominant force at the wall region which smoothed the mean particle velocity and resulted in the almost flat turbulence intensity profiles.

Particle-size distribution

Under the same flow conditions, particles of different sizes may demonstrate completely different hydrodynamic behavior. In this study, the particle mixtures were divided into five groups:

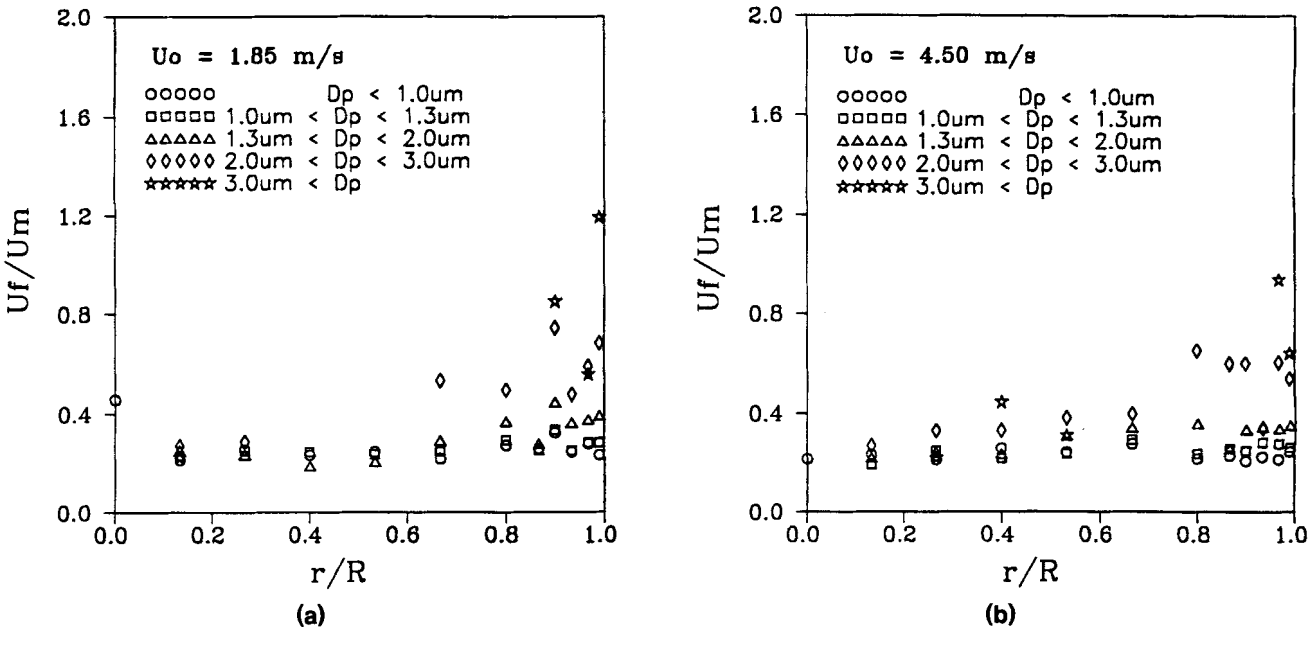

Figure 7. Radial profile of (a) axial turbulent velocity and (b) axial fluctuating velocity of 750 g mixture of 99% shale particles of different sizes and 1% Larostat particles at superficial gas velocity of: (a) 1.85 m/s; (b) 4.50 m/s.

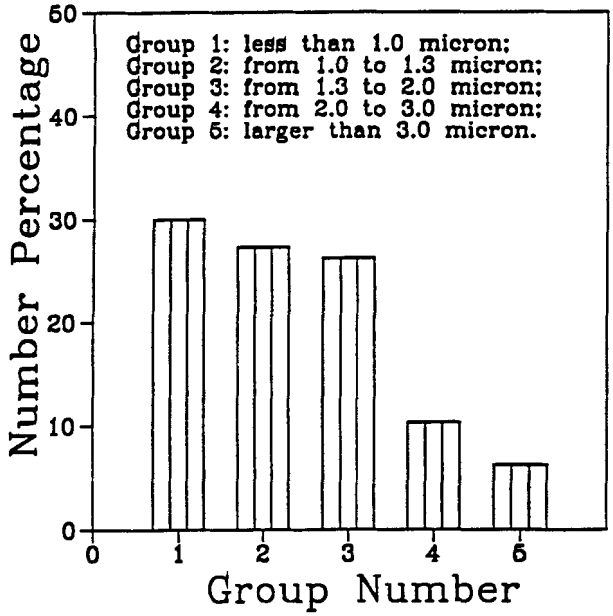

Figure 8. Initial shale particle-size distribution measured by Malvern instrument.

Group 1: less than 1.0 μm
Group 2: from 1.0 to 1.3 μm
Group 3: from 1.3 to 2.0 μm
Group 4: from 2.0 to 3.0 μm
Group 5: larger than 3.0 μm.

The reference particle-size distribution measured by a Coulter counter is shown in Figure 8. A minimum amount of agglomeration and cluster formation was expected in the measurements using a Coulter counter.

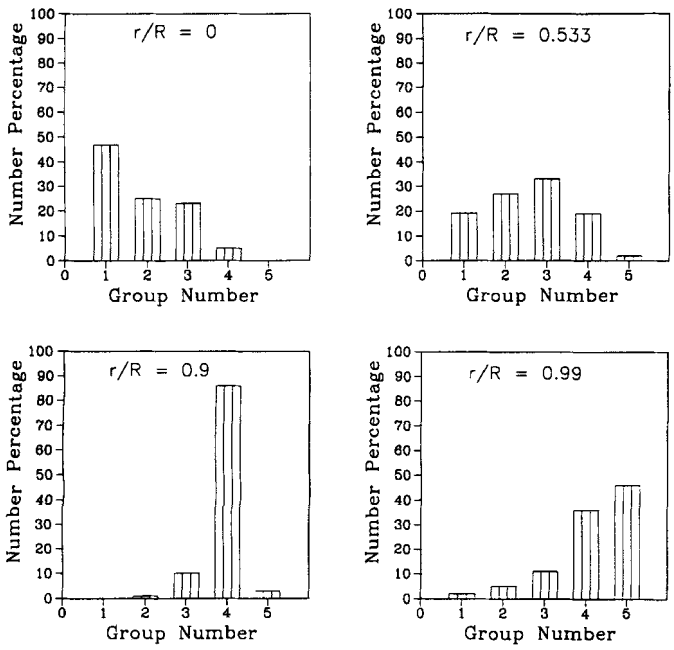

Figure 9. Local shale particle-size distribution of four different radial locations at superficial gas velocity of 1.85 m/s.

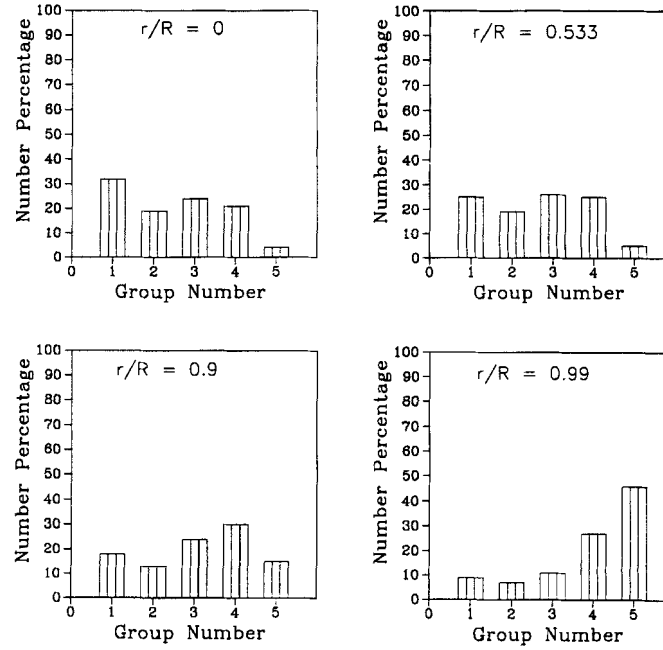

Figure 10. Local shale particle-size distribution of four different radial locations at superficial gas velocity of 4.5 m/s.

Figures 9, 10, 11 and 12 show the local particle-size distribution at four different radial locations at 1.85 and 4.50 m/s superficial gas velocities for shale fines and shale fines with 1% Larostat powder, respectively. Figure 9 shows for the case of 750 g of pure circulating shale fines at 1.85 m/s gas superficial velocity, there exists an annular region in the vicinity of

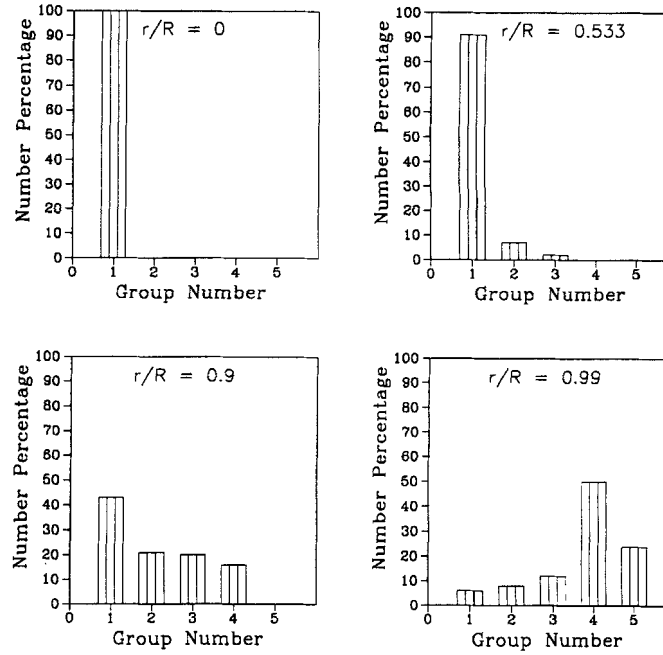

Figure 11. Local particle-size distribution of mixture of 99% shale particles and 1% Larostat particles at four different radial locations at superficial gas velocity of 1.85 m/s.

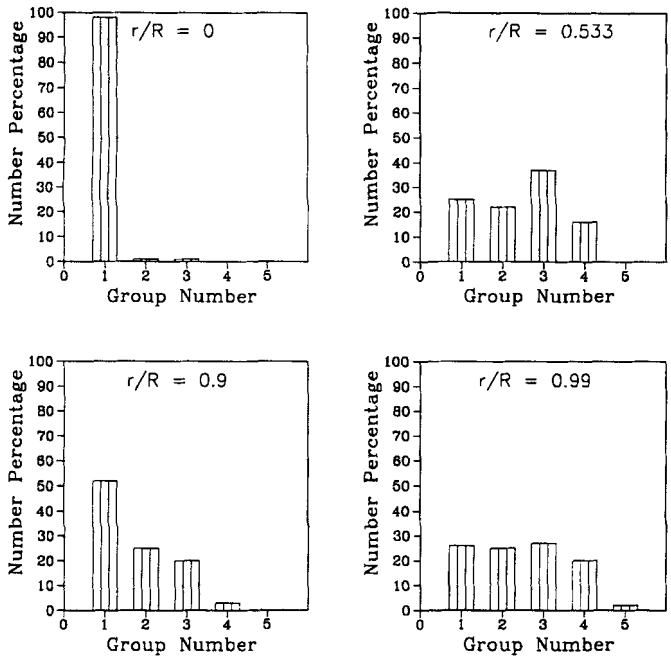

Figure 12. Local particle-size distribution of mixture of 99% shale particles and 1% Larostat particles at four different radial locations at superficial gas velocity of 4.5 m/s.

the wall where more than 80% of the particles are larger than 2.0 microns, while, in the core region, about 95% of the particles are less than 2.0 microns. Figure 10 also shows a similar variation of the annular flow structure for the case of 750 g of pure circulating shale fines at 4.5 m/s. The radial particle-size distribution for higher gas superficial velocities was smoother, mainly due to enhanced particle collision as a result of the more chaotic flow patterns at higher gas velocities. At 4.5 m/s superficial gas velocities, about 75% of the particles at the center are smaller than 2.0 microns in comparison with 95% at lower gas velocities. In addition, at the wall, 70% of the particles are larger than 2.0 microns in comparison with 80% at the lower gas velocities. The percentage of smaller particles at the wall region and larger particles at the central region was enhanced with increased gas velocities as a result of the increase in turbulence behavior and particle collision. In the wall region, the average particle size always reached the maximum value at the locations close to the wall ($r/R = 0.99$) at all superficial gas velocities. This could be partly due to the particle collision with the wall having a different restitution coefficient than the particles; lower particle velocities and fluctuating velocities; and higher electrostatic force near the wall. In some cases, instantaneous downflow of the particles and very high solid volumetric concentration were observed at the wall region. Our data showed that low velocities and fluctuating velocities result in the formation of clusters and agglomerates which are more stable. In other words, the larger fluctuating velocity continuously breaks the big clusters and, in turn, results in continuous oscillation of particle-size distribution. Wide particle-size distribution was observed at higher superficial gas velocities due to significant mixing, turbulence, and extensive agglomeration and deagglomeration. However, at a constant superficial gas velocity, more large particles or agglomerates were obtained in the wall region and the particle sizes gradually increased with r/R.

For shale fines with 1% Larostat powder, almost no clusters or agglomerates were obtained even at the wall region.

Figure 11 shows the particle-size distribution at different radial locations at a gas velocity of 1.85 m/s using a mixture of fine shales and 1% Larostat powder. Less than 25% of particles larger than 3 microns were obtained at the wall in comparison to about 45% under similar conditions without Larostat powder. This result shows the significant contribution of 1% Larostat powder in reducing interparticle (electrostatic) force, even at the wall region. A considerable separation of particles of different sizes was observed using 1% Larostat powder, particularly at the center of the pipe, where all the particles were less than 1 micron.

Figure 12 shows the particle-size distribution at different radial locations at 4.5 m/s gas velocity using a mixture of fine shales and 1% Larostat powder. The particle-size distribution showed intensity similar to the case with lower gas velocity. The major difference was that less than 5% of particles larger than 3 μm was observed at the locations except the wall region. The major contribution of 1% Larostat powder near the wall at 4.5 m/s gas velocity was a significant reduction in electrostatic force due to the collision of fine shale particles with the Larostat powder, which significantly reduced the percentage of particles bigger than 3 μm.

The effects of superficial gas velocity on overall particle size are shown in Figure 13. For pure shale fines, the size range of the number average particle size without 1% Larostat was between 1.5 to 3.5 μm at all gas superficial veloci-

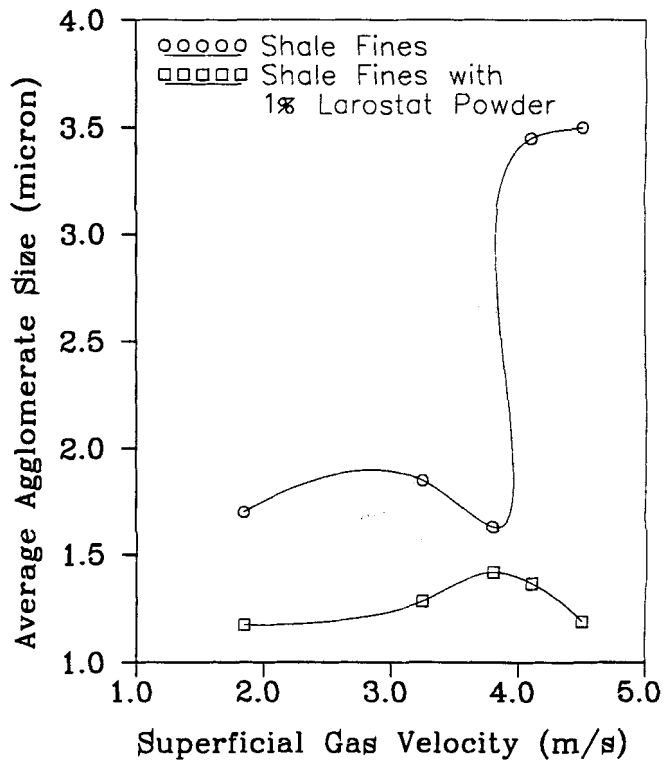

Figure 13. Effect of superficial gas velocity on average size of agglomerates or clusters of shale particles with or without Larostat particles.

ties. When superficial gas velocity was increased, the overall average particle size was first increased slightly due to an increase in the collision frequency; then it decreased which indicated the deagglomeration process became effective at a certain superficial gas velocity. After this critical superficial gas flow rate, the agglomeration process became dominant again and resulted in the significant increase in the average particle size. We believe at the higher superficial gas velocities, an increase in the frequency of collisions of the particles, local eddies, and streaming of the particles (many particles following each other in the same stream line) may significantly contribute to the formation of more agglomerates and clusters.

For shale fines with 1% Larostat powder, the size range of the number average particle size was between 1.2 to 1.4 μm for all gas superficial velocities. The overall number average particle sizes in the riser were about the same at different superficial gas velocities. This means only an insignificant amount of agglomerates was formed in the presence of Larostat powder. In general, the number average particle size slightly increased at lower superficial gas velocities; then, at a critical superficial gas velocity, the particle sizes decreased with increasing superficial gas velocities. The critical superficial gas velocity for our experiment was between 3.30 and 3.80 m/s. By adding Larostat powder, the overall average particle size significantly decreased and the formation of agglomerates, which was caused by high superficial gas velocity effects, was eliminated. Therefore, the shale particles which belong to Group C acted similar to Group A and B particles.

Maxwellian distribution of particles

Ogawa et al. (1980) suggested that the mechanical energy of granular flow is first transformed into random particle motion and then dissipated into internal energy. Savage and Jeffrey (1983) related the fluctuating velocity to the absolute value of the shear gradient and concluded that the dense-phase kinetic theory may be applied to particle flow systems. Later on, the kinetic theory approach to gas/solid systems was used by many investigators including Gidaspow (1994), Sinclair and Jackson (1989), and Arastoopour and Kim (1994).

In this study, we used our data on instantaneous particle velocities at different locations and operating conditions for gas/dilute shale particles with and without antistatic agents and compared the results with the Maxwellian (normal) distribution function. This means that the particles oscillate about the mean values in a chaotic manner. The one-dimensional Maxwellian or normal distribution function may be expressed as

$$f_{\text{Maxwell}}(u_p) = \frac{1}{(2\pi\theta)^{1/2}} \exp\left[-\frac{(u_p - u_m)^2}{2\theta}\right]$$

where u_m is mean velocity and θ is defined as granular temperature or standard deviation and

$$u_m = \int_{-\infty}^{+\infty} u_p f_{\text{exp}}(u_p) du_p$$

$$\theta = \int_{-\infty}^{+\infty} (u_p - u_m)^2 f_{\text{exp}} u_p du_p$$

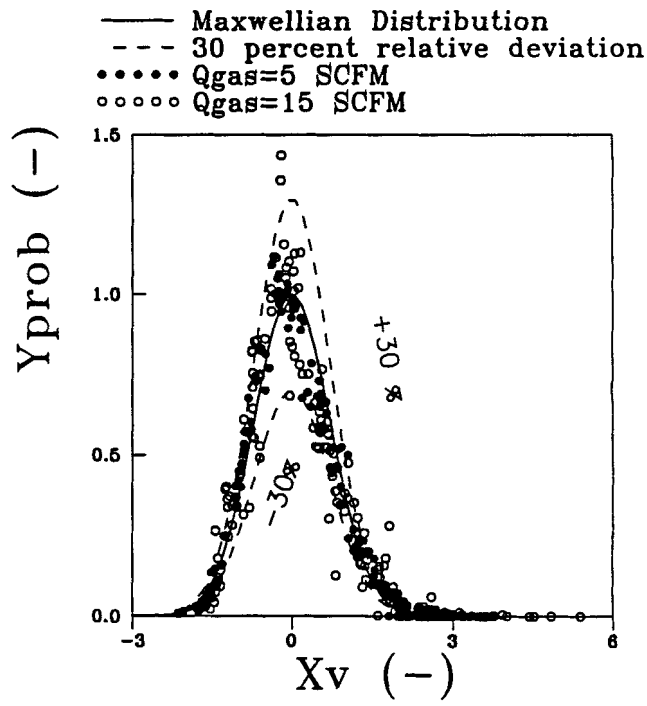

Figure 14. Comparison of Maxwellian distribution with actual probability density obtained using our experimental data.

where $f_{\text{exp}}(u_p)$ is the velocity probability density function obtained based on our experimental data. In order to clarify the derivation of the Maxwellian distribution from the experimental data, we define

$$X_V = \frac{u_p - u_m}{\sqrt{2\theta}}$$

$$Y_{\text{Prob}} = \sqrt{2\pi\theta} f(u_p)$$

Thus the Maxwellian distribution may be written as

$$Y_{\text{Prob}} = \exp(-X_V^2)$$

Figure 14 shows the comparison of velocity probability predicted by Maxwellian distribution with our experimental data for shale particles. Adding Larostat powder resulted in a distribution function closer to Maxwellian; however, it did not significantly change the velocity probability distribution. The deviation is within $\pm 30\%$ which clearly indicates that it is reasonable to assume that the particles oscillate about the mean values in a rather chaotic manner. In other words, the kinetic theory approach, even for cohesive particles, is a very good approximation for describing complicated gas/particle flow systems.

Conclusions

For shale fines (Group C particles), average particle size increased at higher superficial gas velocities due to significant mixing and particle collision which resulted in extensive

agglomeration. The overall average particle size did not always increase with an increase in superficial gas velocity. At constant superficial gas velocity, more large particles and agglomerates (clusters) with very small or, in some cases, negative instantaneous velocities were observed in the wall vicinity. The mean particle velocities showed two peaks located at $r/R = 0$ and $r/R = 0.55$ at lower superficial gas velocities; however, at higher superficial gas velocities, the particle velocity profiles showed a parabolic shape. This could be due to significant particle collision and higher drag force exerted by gas on the particles which, in turn, resulted in more homogeneous flow of particles. This velocity profile is similar to the average particulate phase velocity profile. In the wall region, the fluctuating velocities were always lower than those in the core region, although the turbulence intensities were much higher in the wall region.

By adding 1% Larostat powder to the shale fines, the overall average particle size did not change significantly. The velocity profiles of the small particles were almost flat and only the large particle velocities decreased slightly near the wall. A plug-flow profile for particle velocities was obtained at high superficial gas velocities. The flat profiles were also obtained for particle fluctuating velocities. Overall, the 1% Larostat powder significantly reduced interparticle (electrostatic) force and, in turn, made particles of Group C behave similar to Group A particles or, in some cases, to Group B particles.

Based on experimental data on instantaneous velocities of shale particles with or without antistatic agents in a dilute gas/solid system, it is reasonable to assume that the particles oscillate about the mean values in a chaotic manner. Therefore, the velocity distribution may be approximated by the Maxwellian distribution function and kinetic theory is a very promising approach to describe gas/particle flow systems.

Notation

N_{sample} = sample number
r = radial location
R = radius of pipe
U_o = superficial gas velocity
U_p = particle local velocity

Literature Cited

Arastoopour, H., and H. S. Kim, "Numerical Analysis of Dilute Gas Particles Flow Using the Kinetic Theory," *Parallel Computing in Multiphase Flow Systems Simulation*, S. Kim, G. Karniadakis, and M. K. Vernon, eds., Vol. 199, No. G00899, ASME, New York (1994).

Arastoopour, H., and Y. Yang, "Experimental Studies on Dilute Gas and Cohesive Particles Flow Behavior Using Laser Doppler Anemometer," *Fluidization VII*, O. E. Potter, and D. J. Nicklin, eds., Engineering Foundation, New York, p. 723 (1991).

Farmer, W. M., "Measurement of Particle Size and Concentration Using LDV Techniques," *Proc. Dynamic Flow Conf.* (1978).

Geldart, D., "Types of Gas Fluidization," *J. Powder Technol.*, **7**, 285 (1973).

Gidaspow, D., *Multiphase Flow and Fluidization*, Academic Press, San Diego, CA (1994).

Jones, T. B., and D. J. King, *Powder Handling and Electrostatics*, Lewis Publishing, MI (1991).

Lesinski, J., B. Mizera-Lesinska, J. C. Fanton, and M. I. Boulos, "Laser Doppler Anemometry Measurements in Gas-Solid Flows," *AIChE J.*, **27**, 358 (1981).

Ogawa, S., A. Umemura, and N. Oshima, "On the Equations of Fully Fluidized Granular Materials," *J. Appl. Math. Phys.*, **31**, 483 (1980).

Reddy, K. V. S., "Particle Dynamics in Solid-Gas Flow in Vertical Dust," PhD Diss., Univ. of Waterloo (1967).

Savage, S. B., and D. J. Jeffrey, "The Stress Tensor in a Granular Flow at High Shear Rates," *J. Fluid Mech.*, **194**, 457 (1983).

Sinclair, J. L., and R. Jackson, "Gas-Particle Flow in a Verticle Pipe with Particle-Particle Interaction," *AIChE J.*, **35**, 1473 (1989).

Soo, S. L., G. J. Treyek, R. C. Dimick, and G. F. Hohnstreiter, "Concentration and Mass Flow Distribution in a Gas-Solid Suspension," *I&EC Fund.*, **3**(2), 98 (1964).

Tsuji, Y., and Y. Morikawa, "LDV Measurements of an Air-Solid Two-Phase Flow in a Horizontal Pipe," *J. Fluid Mech.*, **120**, 385 (1981).

Tsuji, Y., Y. Morikawa, and H. Shiomi, "LDV Measurements of an Air-Solid Two-Phase Flow in a Vertical Pipe," *J. Fluid Mech.*, **139**, 417 (1984).

Yang, Y.-L., Y. Jin, Z.-A. Yu, Z.-W. Wang, and D. Bai, "The Radial Distribution of Local Particle Velocity in a Dilute Circulating Fluidized Bed," *Proc. Int. Conf. Circulating Fluidized Beds*, P. Basu, M. Horia, and M. Hasatani, eds., Pergamon Press, New York, p. 201 (1990).

Yang, Y., "Experiments and Theory on Gas and Cohesive Particles Flow Behavior and Agglomeration in the Fluidized Bed Systems," PhD Diss., Illinois Inst. of Technol., Chicago (1991).

Zhang, Y.-F., "Particles Flow Behavior in the Riser of a Circulating Fluidized Bed," PhD Diss., Illinois Inst. of Technol., Chicago (1992).

Zhang, Y.-F., and H. Arastoopour, "Dilute FCC Particles/Gas Flow Behavior in the Riser of a Circulating Fluidized Bed," *Powder Technol. J.*, **84**(3) (1995).

Manuscript received Apr. 3, 1995, and revision received Aug. 25, 1995.